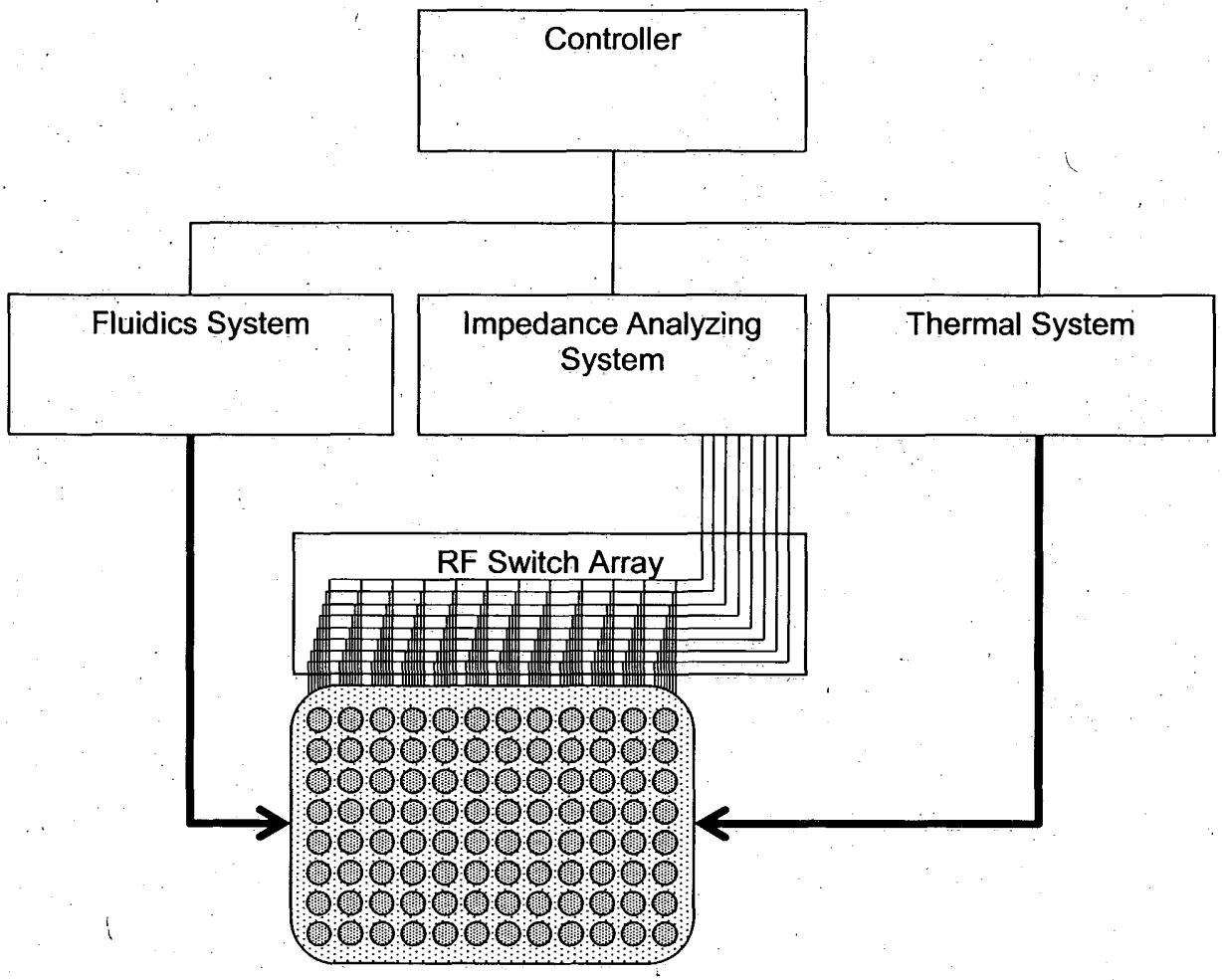

Figure 1a. A block diagram that illustrates one embodiment of the bioimpedance measuring system.

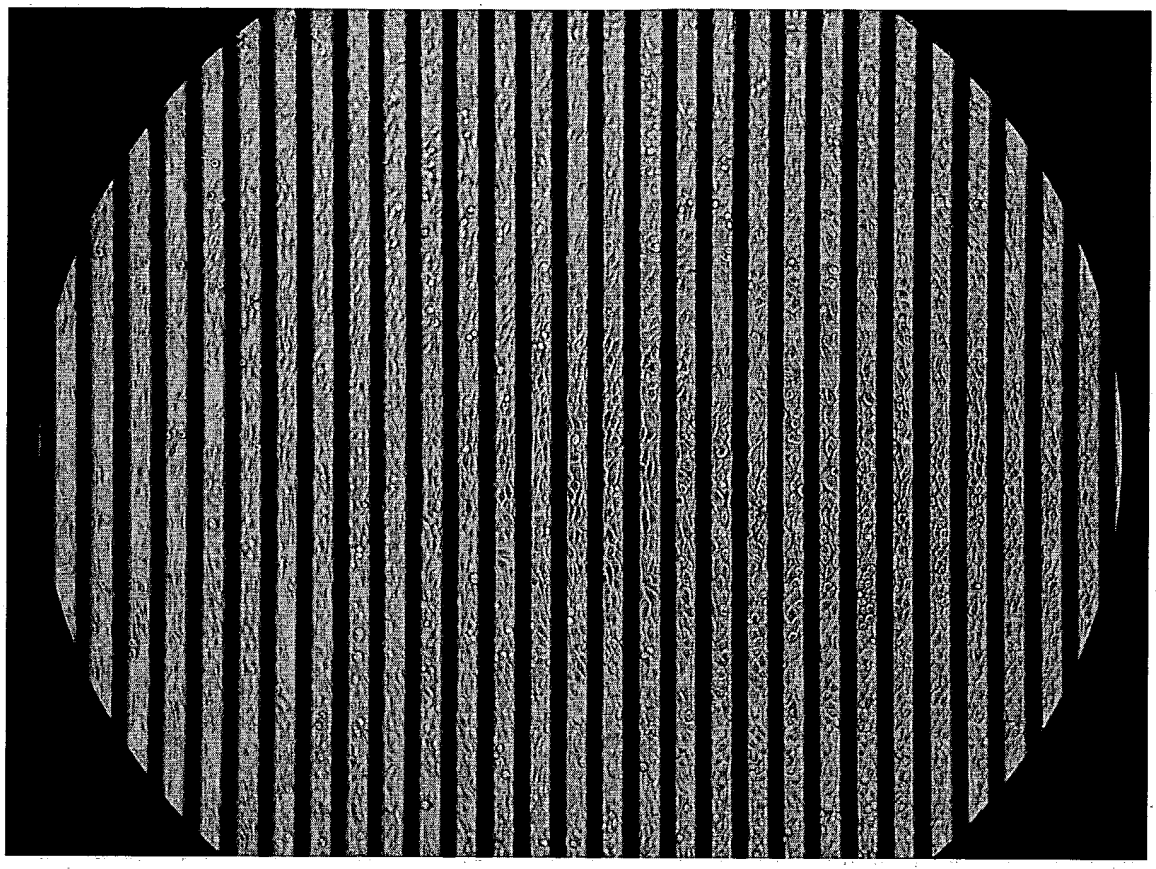

Figure 1b. The bioimpedance system displaying cells on the inter-digitated electrodes of a micro-titre plate well.

Figure 2

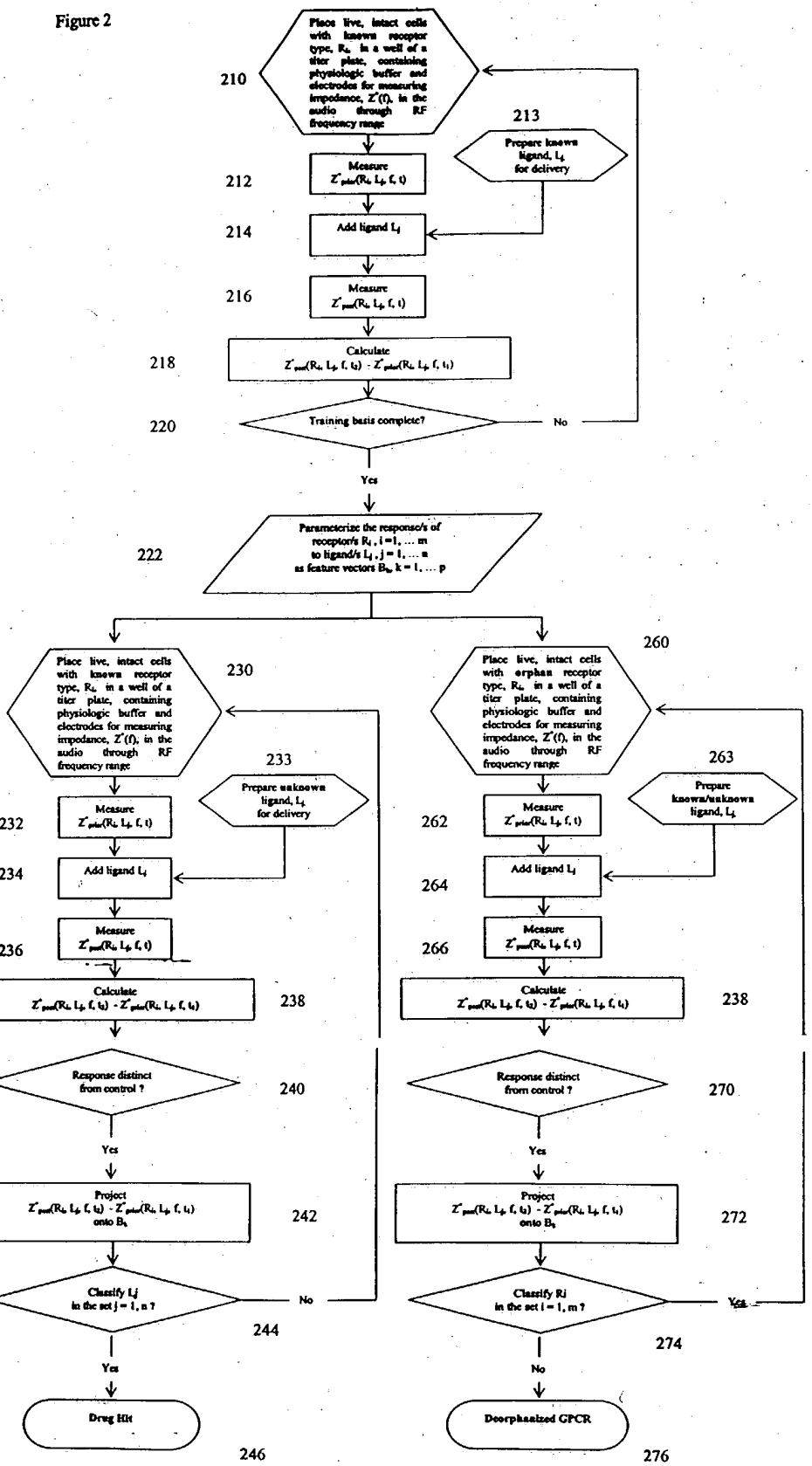
Place live, intact cells with known receptor type, R_i, in a well of a titer plate, containing physiologic buffer and electrodes for measuring impedance, $Z'(f)$, in the audio through RF frequency range
210
213
Prepare known ligand, L_j for delivery
Measure $Z'_{prior}(R_i, L_j, f, t)$
212
Add ligand L_j
214
Measure $Z'_{post}(R_i, L_j, f, t)$
216
Calculate $Z'_{post}(R_i, L_j, f, t_2) - Z'_{prior}(R_i, L_j, f, t_1)$
218
Training basis complete?
220
No
Yes
Parameterize the response/s of receptor/s R_i, $i = 1, \ldots m$ to ligand/s L_j, $j = 1, \ldots n$ as feature vectors B_k, $k = 1, \ldots p$
222
Place live, intact cells with known receptor type, R_i, in a well of a titer plate, containing physiologic buffer and electrodes for measuring impedance, $Z'(f)$, in the audio through RF frequency range
230
233
Prepare unknown ligand, L_j for delivery
Measure $Z'_{prior}(R_i, L_j, f, t)$
232
Add ligand L_j
234
Measure $Z'_{post}(R_i, L_j, f, t)$
236
Calculate $Z'_{post}(R_i, L_j, f, t_2) - Z'_{prior}(R_i, L_j, f, t_1)$
238
Response distinct from control ?
240
Yes
Project $Z'_{post}(R_i, L_j, f, t_2) - Z'_{prior}(R_i, L_j, f, t_1)$ onto B_k
242
Classify L_j in the set $j = 1, n$?
No
244
Yes
Drug Hit
246
Place live, intact cells with orphan receptor type, R_i, in a well of a titer plate, containing physiologic buffer and electrodes for measuring impedance, $Z'(f)$, in the audio through RF frequency range
260
263
Prepare known/unknown ligand, L_j
Measure $Z'_{prior}(R_i, L_j, f, t)$
262
Add ligand L_j
264
Measure $Z'_{post}(R_i, L_j, f, t)$
266
Calculate $Z'_{post}(R_i, L_j, f, t_2) - Z'_{prior}(R_i, L_j, f, t_1)$
238
Response distinct from control ?
270
Yes
Project $Z'_{post}(R_i, L_j, f, t_2) - Z'_{prior}(R_i, L_j, f, t_1)$ onto B_k
272
Classify R_i in the set $i = 1, m$?
Yes
274
No
Deorphanized GPCR
276

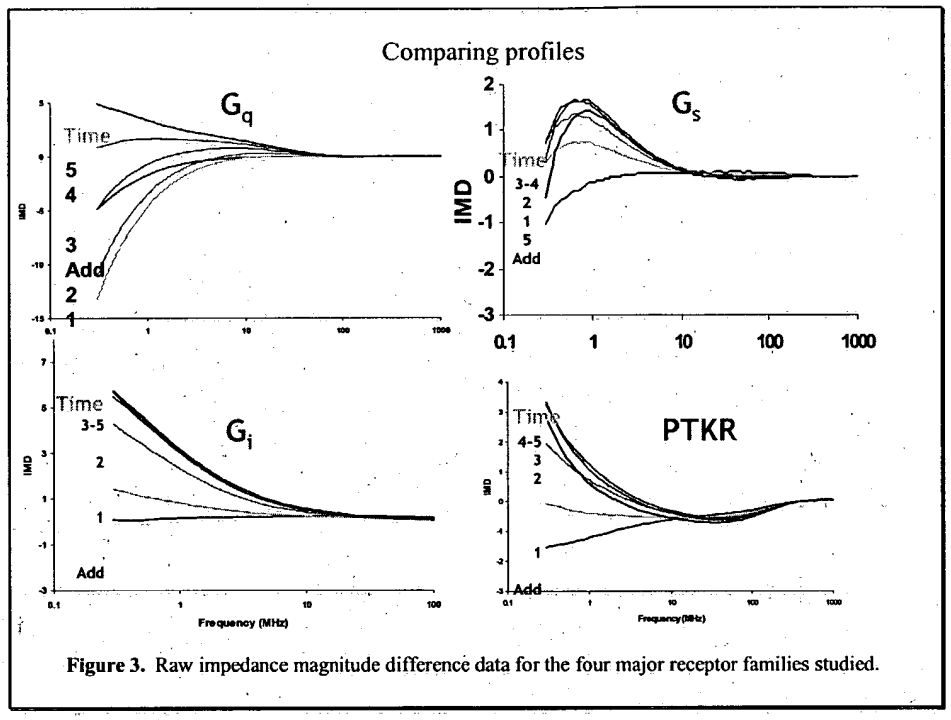

Figure 3. Raw impedance magnitude difference data for the four major receptor families studied.

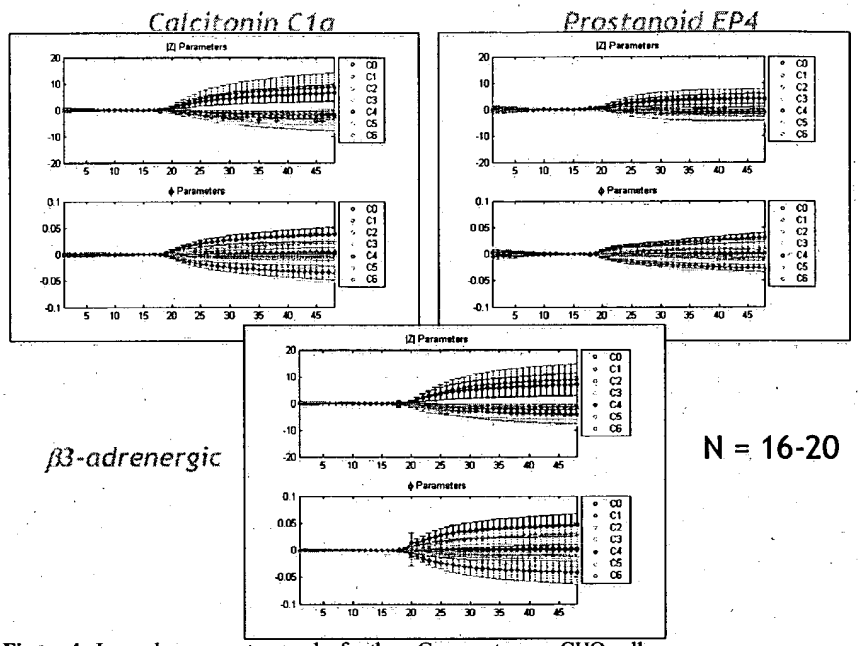

Figure 4. Legendre parameter graphs for three Gs receptors on CHO cells.

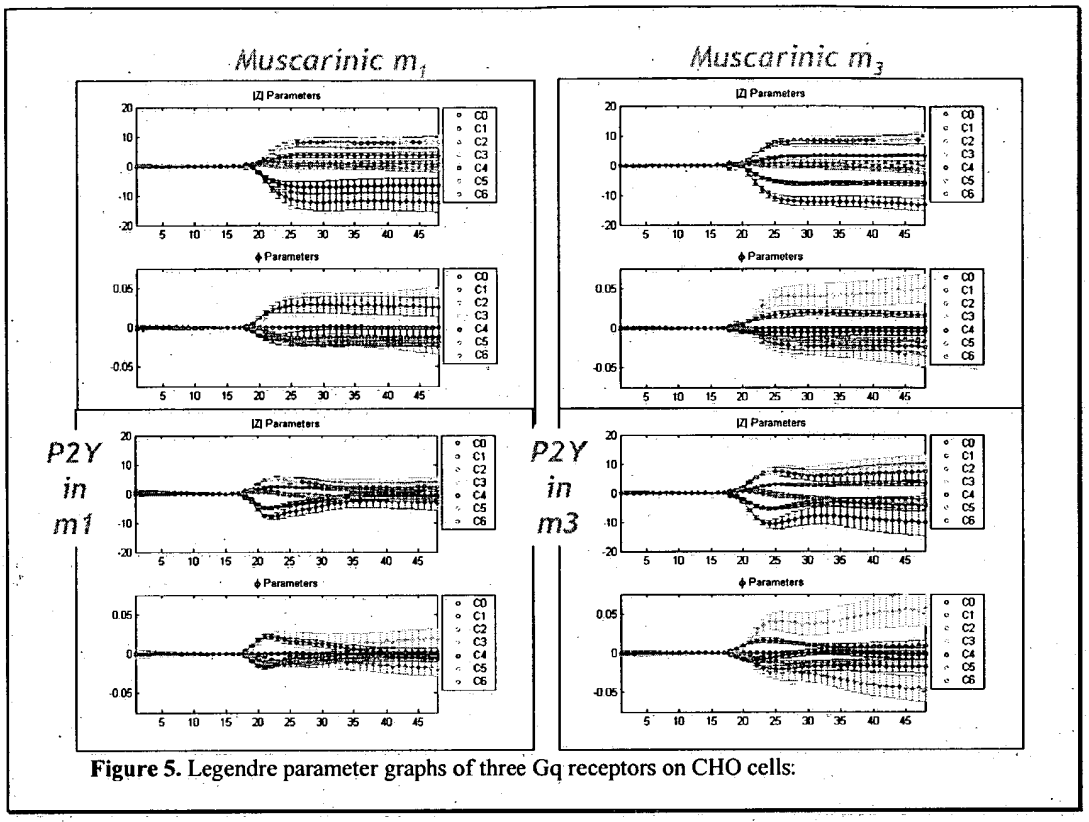

Figure 5. Legendre parameter graphs of three Gq receptors on CHO cells:

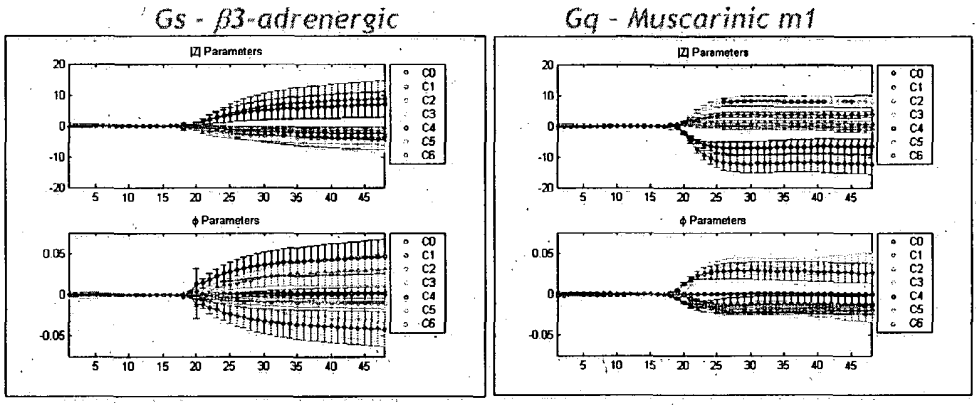

Figure 6. Comparison of parameter graphs for Gs and Gq receptors on CHO cells.

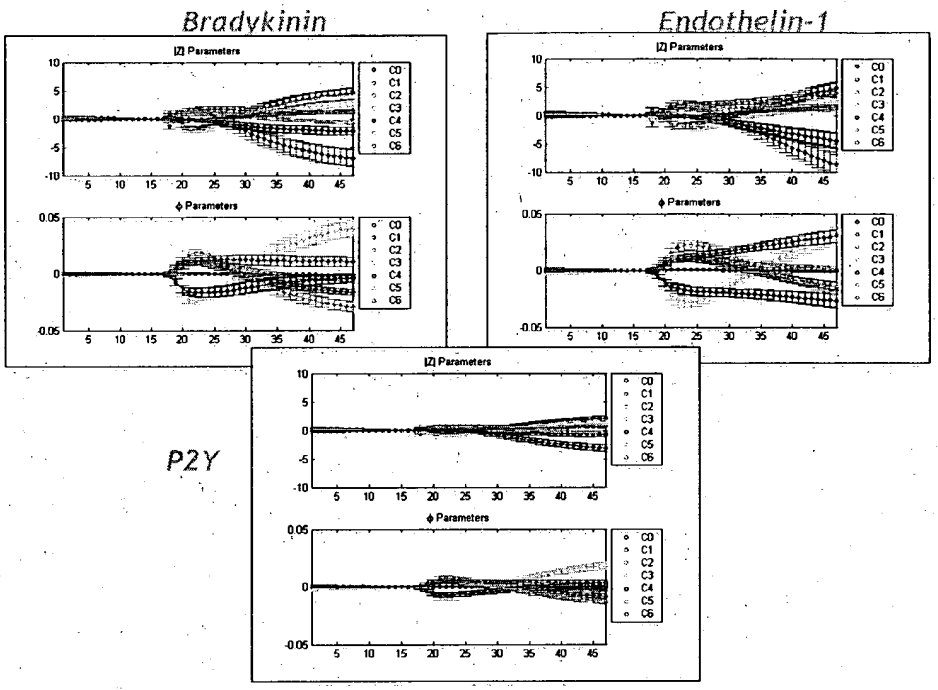

Figure 7. Legendre parameter graphs for three Gq receptors on HeLa cells.

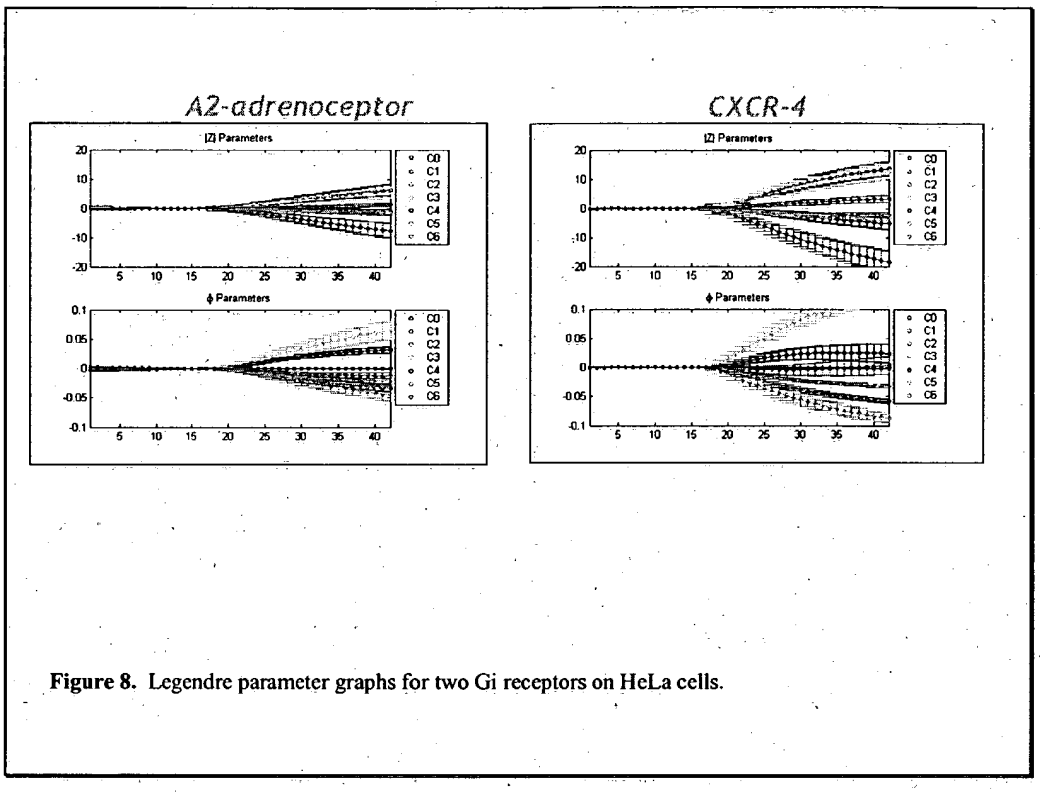

Figure 8. Legendre parameter graphs for two Gi receptors on HeLa cells.

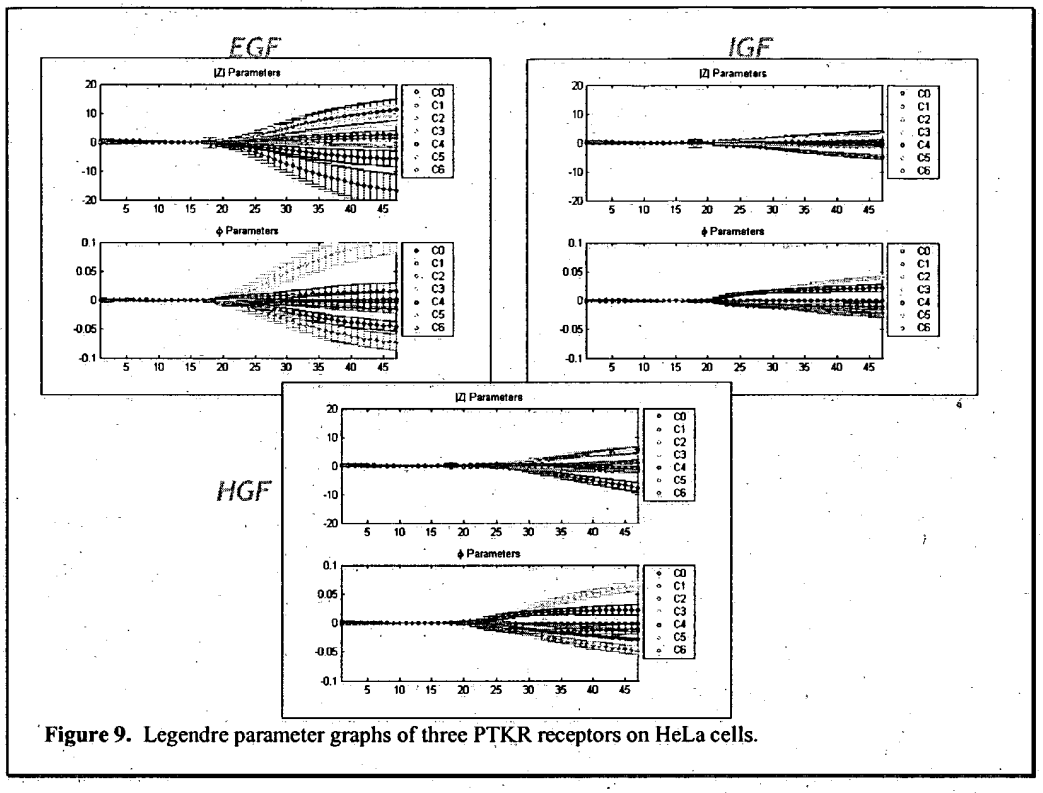

Figure 9. Legendre parameter graphs of three PTKR receptors on HeLa cells.

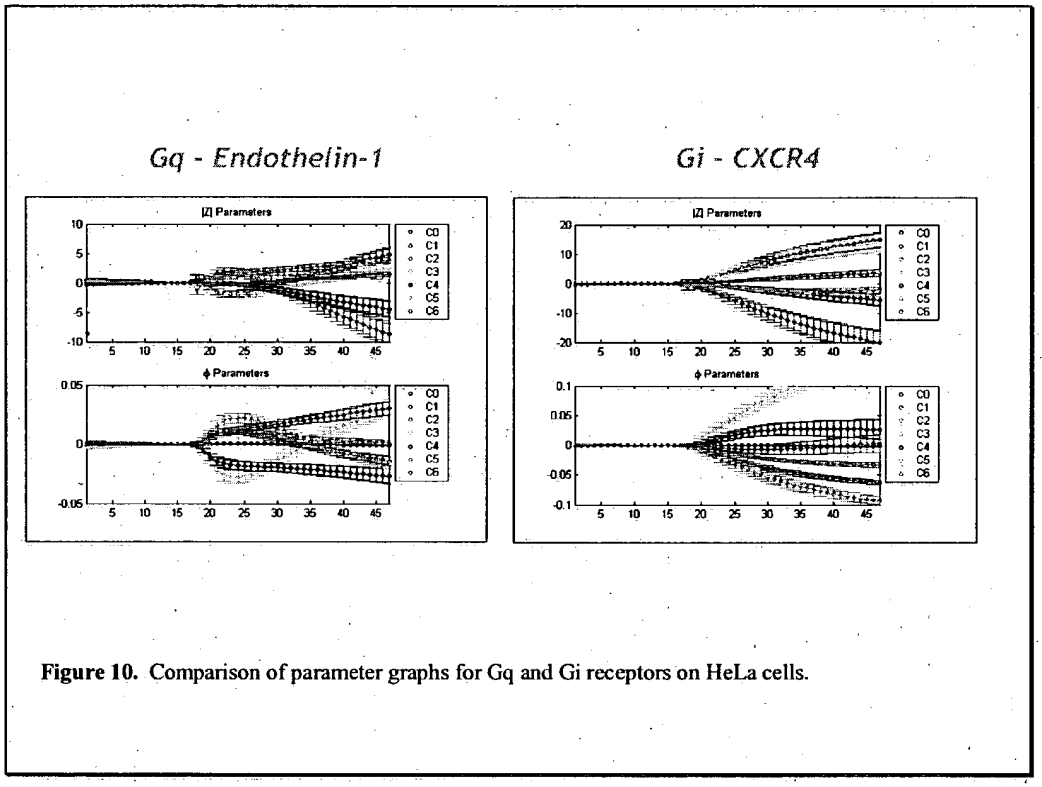

Figure 10. Comparison of parameter graphs for Gq and Gi receptors on HeLa cells.

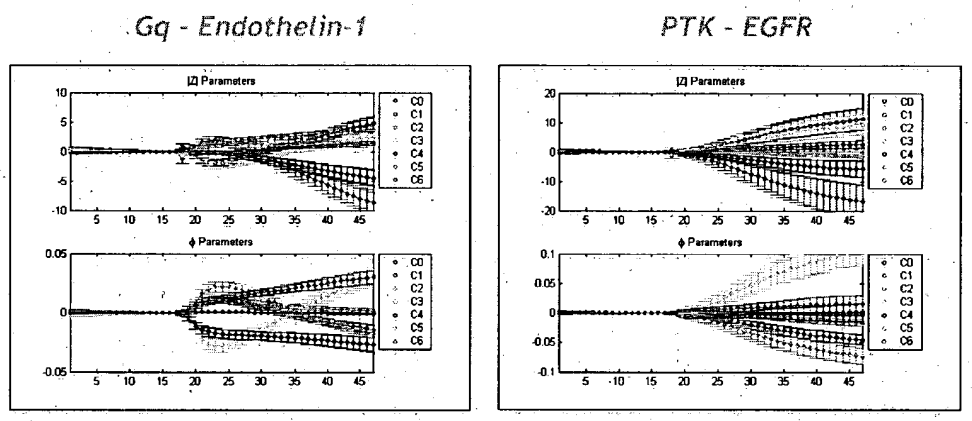

Figure 11. Comparison of parameter graphs for Gq and PTKR receptors on HeLa cells.

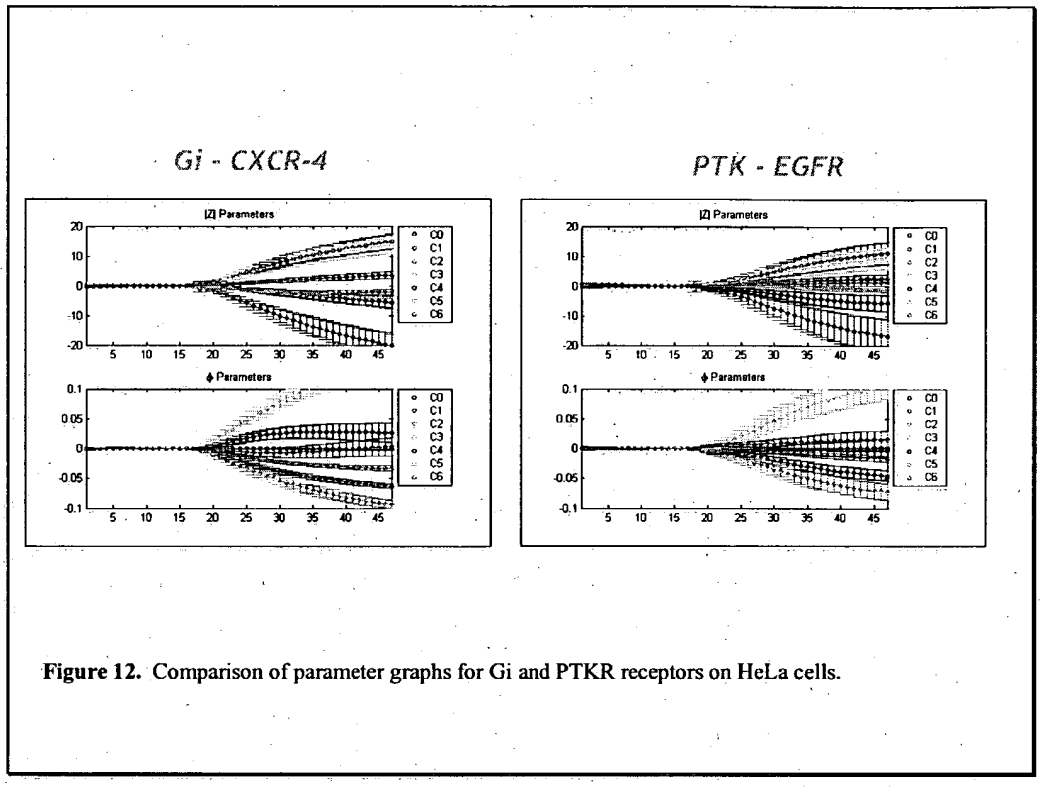

Figure 12. Comparison of parameter graphs for Gi and PTKR receptors on HeLa cells.

|Z| QDS	Predicted Membership					% error
		Buffer	Gq (m1)	Gs (β3)	Gi (k1)	
Actual Membership	Gq	0	77	0	0	0.0
	Gs	0	0	44	2	4.3
	Gi	0	3	0	33	8.3

total error
3.1 %

ϕ QDS	Predicted Membership					% error
		Buffer	Gq (m1)	Gs (β3)	Gi (k1)	
Actual Membership	Gq	0	77	0	0	0.0
	Gs	0	0	45	1	2.2
	Gi	0	7	2	27	25.0

total error
6.3 %

Figure 13. Analysis matrix showing results of standard multidimensional data classification using the confusion matrix technique on data from CHO cells.

|Z|	Predicted Membership					% error
Actual Membership		Buffer (SV)	Gi	Gq	PTK	
	Buffer (SV)	42	1	1	1	6.7
	Gi	0	46	0	0	0.0
	Gq	0	0	36	0	0.0
	PTK	3	1	0	37	9.8

total error
4.2 %

ϕ	Predicted Membership					% error
Actual Membership		Buffer (SV)	Gi	Gq	PTK	
	Buffer (SV)	40	0	1	4	11.1
	Gi	0	46	0	0	0.0
	Gq	0	0	36	0	0.0
	PTK	1	2	0	38	7.3

total error
4.8 %

Figure 14. Analysis matrix showing results of standard multidimensional data classification using the confusion matrix technique on data from HeLa cells.